Chapter 2

RNA Structure Determination by NMR

Lincoln G. Scott and Mirko Hennig

Abstract

This chapter reviews the methodologies for RNA structure determination by liquid-state nuclear magnetic resonance (NMR). The routine production of milligram quantities of isotopically labeled RNA remains critical to the success of NMR-based structure studies. The standard method for the preparation of isotopically labeled RNA for structural studies in solution is *in vitro* transcription from DNA oligonucleotide templates using T7 RNA polymerase and unlabeled or isotopically labeled nucleotide triphosphates (NTPs). The purification of the desired RNA can be performed by either denaturing polyacrylamide gel electrophoresis (PAGE) or anion-exchange chromatography. Our basic strategy for studying RNA in solution by NMR is outlined. The topics covered include RNA resonance assignment, restraint collection, and the structure calculation process. Selected examples of NMR spectra are given for a correctly folded 30 nucleotide-containing RNA.

Key words: RNA, RNA synthesis, RNA purification, NMR, resonance assignment, structure determination.

1. Introduction

RNA continues to surprise the scientific community with its rich structural diversity and unanticipated biological functions, including catalysis and the regulation of gene expression. Knowledge of the three-dimensional structure of biological macromolecules is indispensable for describing and understanding the underlying determinants of molecular recognition. RNA-ligand recognition generally occurs by "induced-fit" rather than by rigid "lock-and-key" docking *(1, 2)*. These recognition processes apparently necessitate conformational flexibility for which liquid state NMR spectroscopy is uniquely suited to answer important questions in this area by looking at dynamic ensembles of structures.

Jonathan M. Keith (ed.), *Bioinformatics, Volume I: Data, Sequence Analysis, and Evolution, vol. 452*

Book doi: 10.1007/978-1-60327-159-2 Springerprotocols.com

Large quantities of RNA can be routinely prepared from either DNA template-directed *in vitro* transcription using T7 RNA polymerase (as well as T3 or SP6), or phosphoramidite-based chemical synthesis. This chapter focuses on the *in vitro* transcription method using T7 RNA polymerase, which is both more efficient, and cost effective (especially for RNAs >50 nucleotides) *(3, 4)*. However, the disadvantages of *in vitro* transcription include difficulties associated with the selective incorporation of isotopically labeled nucleotides or modified nucleotides, which are often functionally important.

The proliferation of RNA structure determinations using NMR spectroscopy is the combined result of:

1. The availability of efficient methods for isotopic labeling of RNA molecules, which permits heteronuclear experiments to be performed that resolve the severe spectral overlap inherent in proton spectra of RNAs
2. The rapid development of pulse sequences tailored for RNA spin systems facilitating many structure determinations

Severe spectral overlap in unlabeled RNA seriously limits the application of solution studies by NMR (**Fig. 2.1**). In contrast to the abundant ^{1}H isotope, the naturally occurring nuclei ^{12}C and ^{14}N cannot be readily studied with high-resolution NMR techniques. The production of isotopically labeled RNA remains critical to the success of these NMR-based structure studies *(5)* and a variety of synthetic methods have been developed for the routine production of isotopically labeled nucleotides. Labeled NTPs for *in vitro* transcription reactions can be readily produced

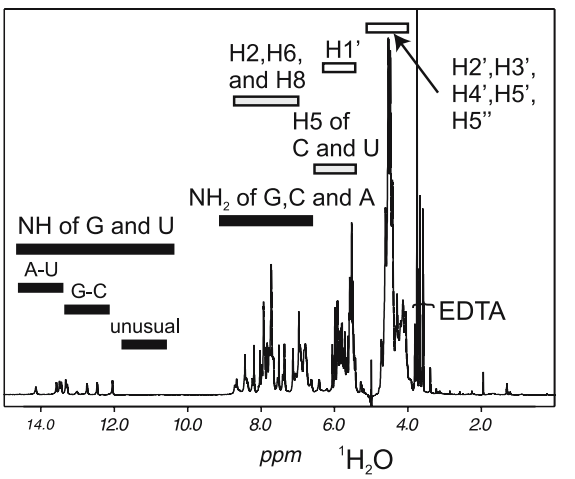

Fig. 2.1. 1D ^{1}H spectrum of the 30 nucleotide HIV-2 TAR RNA recorded in H_2O. Typical ^{1}H chemical shift ranges are indicated; solid black bars highlight exchangeable imino and amino protons, gray bars non-exchangeable base, and open bars non-exchangeable ribose protons.

by enzymatic phosphorylation of ribonucleoside monophosphates (NMPs) isolated from bacteria such as *Methylophilus methylotrophus* or *E. coli* grown on ^{13}C- and/or ^{15}N enriched media. Optimized and detailed protocols for the preparation of labeled NTPs are published elsewhere and are not covered in this chapter *(6–9)*. Alternatively, a variety of isotopically labeled NTPs are commercially available (e.g., Cambridge Isotope Labs, Sigma-Aldrich, Spectra Gases). Through the use of ^{13}C and ^{15}N isotopic labeling and multidimensional heteronuclear NMR experiments (**Fig. 2.2**), studies of 15-kDa RNAs are commonplace and recent methodological developments have been reviewed *(10–14)*.

New experiments to measure RNA orientation dependent dipolar couplings *(15–17)* and cross-correlated relaxation rates *(18, 19)* have been developed, providing additional structural information. Furthermore, NMR experiments have been introduced that allow the direct identification of donor and acceptor nitrogen atoms involved in hydrogen bonds *(20, 21)*. The unambiguous identification of hydrogen bonds is important in nucleic acid structure determination, particularly for tertiary structural interactions; in the absence of such direct measurements, hydrogen-bonding partners can be misassigned, which will subsequently impact the precision of the resulting structure. All these recently introduced parameters are especially important for structure determination of RNA due to the low proton density, and because a significant number of protons are potentially involved in exchange processes.

We have applied most of the reviewed methods to the 30-nucleotide human immunodeficiency virus (HIV)-2 transactivation response element (TAR) RNA, one of the best-characterized

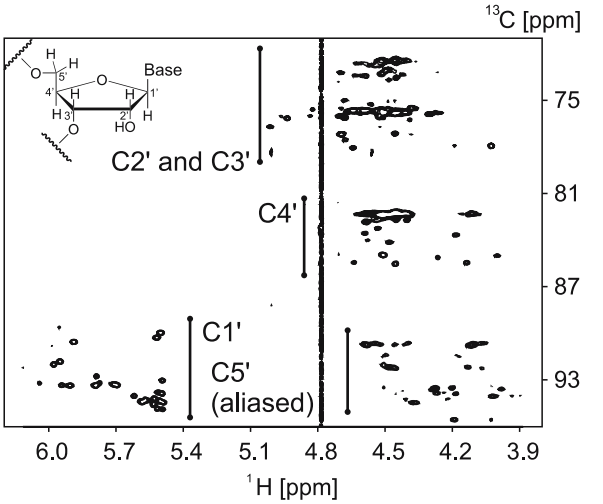

Fig. 2.2. 2D ^{1}H,^{13}C CT-HSQC spectrum of the TAR RNA. Typical ribose ^{13}C chemical shift ranges are indicated. The spectrum was acquired such that the ^{13}C5′ resonances are aliased in ω_1 (–1*spectral width) to improve digital resolution.

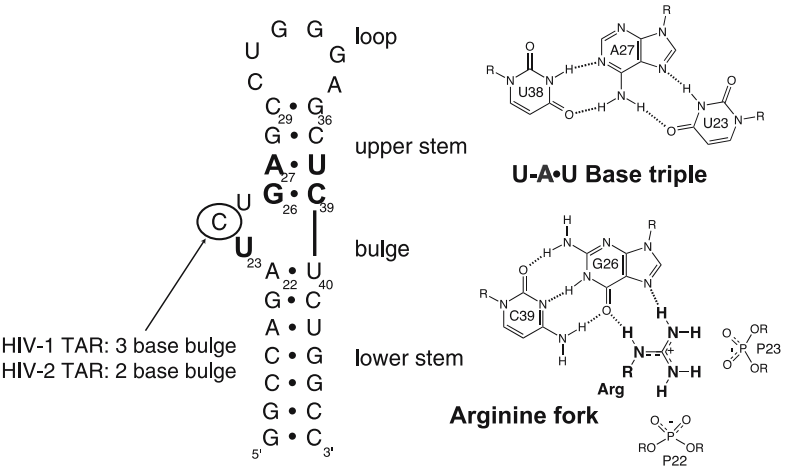

Fig. 2.3. Sequence and secondary structure of the TAR RNA where the bold typeface highlights nucleotides important for Tat recognition. Upon binding of argininamide, the TAR RNA undergoes a conformational change in the bulge region where the essential nucleotides, U38, A27 and U23, form a base triple.

medium-sized RNA molecules. The TAR RNA hairpin loop interacts with Tat, one of the regulatory proteins encoded by HIV. Tat contains an arginine-rich motif responsible for binding to its target *(22, 23)*. Formation of the Tat–TAR interaction is critical for viral replication. Peptides from the basic region of Tat retain the specificity of RNA binding and the amide derivative of arginine also binds specifically to TAR, although with greatly reduced affinity *(24, 25)*. The nucleotides on TAR important for Tat binding are clustered around a three-nucleotide bulge, shown in **Fig. 2.3**. Upon binding of Tat, Tat peptides or argininamide, the TAR RNA undergoes a major conformational change in the bulge region. In the bound form, the essential nucleotides, U38, A27 and U23, form a base triple, shown in **Fig. 2.3**, which results in an opening of the major groove for peptide recognition *(26–29)*. Additional solution studies of the TAR RNA in the absence of ligands have been performed *(30, 31)*.

2. Materials

2.1. In Vitro Transcription

1. Oligonucleotide Transcription Buffer (10×): 800 mM N-(2-hydroxyethyl)-piperazine-N′-2-ethanesulfonic acid potassium salt (K-HEPES), pH 8.1, 10 mM spermidine, and 0.1% (w/v) Triton X-100 prepared in water (*see* **Note 1**).
2. Plasmid Transcription Buffer (10×): 400 mM Tris-HCl, pH 8.1, 10 mM spermidine, 0.1% (w/v) Triton X-100 prepared in water.

3. Solution of 50% (w/v) polyethylene glycol 8000 (PEG-8000) prepared in water.
4. 0.5 M ethylene diamine tetraacetic acid disodium salt (EDTA), pH 8.0, prepared in water *(32)*.
5. TE Buffer: 10 mM Tris-HCl, 1 mM EDTA, pH 8.0, prepared in water.
6. DNA Transcription Promoter Oligonucleotide (60 μM) prepared in water (*see* **Note 2**).
7. DNA Transcription Template Oligonucleotide (60 μM) prepared in water (*see* **Notes 3** and **4**).
8. Linearized Double-Stranded Plasmid DNA Template (≥3 mg/mL) prepared in TE Buffer (*see* **Note 5**).
9. Solutions of 100 mM nucleotide-5′-triphosphates (ATP, UTP, GTP, and CTP) prepared in pH 7.0 water (*see* **Note 6**).
10. Solution of 1 M dithiothreitol (DTT) prepared in water.
11. Solution of 1 M magnesium chloride ($MgCl_2$) prepared in water.
12. Bacteriophage T7 RNA polymerase (*see* **Note 7**).
13. Phenol/chloroform (1:1, v/v; Fisher Scientific) equilibrated with TE buffer.
14. Chloroform/*i*-amyl alcohol (29:1, v/v).
15. Solution of 3 M Sodium Acetate, pH 5.3, prepared in water.
16. 100% Ethanol.
17. 80% Formamide Stop/Loading Buffer (2×): 80% (v/v) formamide, 20% (v/v) 0.5 M (EDTA), pH 8.0, 0.02% (w/v) Bromophenol blue, and 0.02% (w/v) Xylene cyanol prepared in water.
18. 8M Urea prepared in water.

2.2. Polyacrylamide Gel Electrophoresis (PAGE)

1. Twenty Percent Acrylamide/Bisacrylamide Solution: 29:1 (w/w) acrylamide/bisacrylamide, 8 M urea, 90 mM Tris-borate (TBE), 2 mM EDTA, pH 8.1 (*see* **Note 8**).
2. TBE Running Buffer: 90 mM TBE, 2 mM EDTA, pH 8.1, prepared in water.
3. N,N,N′,N′-Tetramethyl-ethylenediamine (TEMED, Bio-Rad) (*see* **Note 9**).
4. Ammonium Persulfate Solution (APS): 30% (w/v) solution in water (*see* **Note 10**).
5. Elutrap Electroelution System (with BT1 and BT2 membranes, Schleicher & Schuell BioScience).
6. CentriPrep concentrator with appropriate molecular weight cut-off (Millipore).

7. NMR Buffer (e.g., 10 mM sodium phosphate, pH 6.5, 50 mM NaCl, 0.1 mM EDTA, 0.02% NaN_3, prepared in 90 % H_2O/10 % D_2O).

2.3. Anion-Exchange Chromatography

1. Low salt loading buffer, e.g., 20 mM potassium phosphate, pH 6.5, 0.5 mM EDTA, 0.02% sodium azide (NaN_3), and 100 mM KCl.
2. High salt elution buffer, e.g., 20 mM potassium phosphate, pH 6.5, 0.5 mM EDTA, 0.02% NaN_3, and 2 M KCl.
3. Two HiTrap Q columns (Amersham Pharmacia).
4. NAP25 column (Amersham Pharmacia).
5. CentriPrep concentrator with appropriate molecular weight cut-off (Millipore).
6. NMR Buffer (e.g. 10 mM sodium phosphate, pH 6.5, 50 mM NaCl, 0.1 mM EDTA, 0.02% NaN_3, prepared in 90 % H_2O/10 % D_2O).

3. Methods

3.1. RNA Sample Preparation and Purification

The yield of *in vitro* transcribed RNA can depend on a variety of factors, many of which are not fully understood. The rational sparse matrix method of duplicate 40–60 conditions in small-scale (10–50 μL) transcription reactions can be easily employed to find the optimal reaction conditions. Trace amounts of α-^{32}P-labeled nucleotide (typically 5.0×10^5:1 [mol/mol] GTP:α-^{32}P-GTP (800 Ci/mmol), Perkin Elmer, Wellesley, MA) can be included to permit later radioanalytic quantitation of the transcription products. After four hours of incubation at 37°C the reactions are quenched with stop/loading buffer, and loaded directly to a 20% (29:1) denaturing polyacrylamide electrophoresis gel. The dried gel is phosphorimaged and the optimal conditions for transcription are chosen. The conditions can be chosen to either maximize the total yield of RNA, or in the case of isotopically labeled nucleotides, to maximize the yield of RNA per mole of input nucleotides. In addition, computational methods can assist in the interpretation of the experimental transcription optimization data *(33)*. Typically, before embarking on a large-scale synthesis, a pilot 1 mL transcription reaction is carried out to verify the isolated yield. Transcription reactions are carried out on a scale of 1–40 mL, and typical isolated yields are 1–10 nmol RNA per mL of transcription.

Two strategies are available for preparing large quantities of RNA by *in vitro* run-off transcription *(3, 4)*. Transcriptions for short RNAs (< 50 nucleotides) are carried out from synthetic

DNA templates. The non-coding (top) strand and the template strand are purchased and gel purified on at least a 1-μmol scale for large-scale preparations. The preparation of RNA by standard *in vitro* run-off transcriptions from synthetic DNA templates using T7 polymerase becomes inefficient if the RNA transcript is longer than ~60 nucleotides. Thus, larger RNA transcripts are typically synthesized using linearized plasmid DNA containing the target RNA coding sequence under a T7 promoter (**Fig. 2.4**).

RNA structural studies in solution by NMR require milligram amounts of the desired RNA of specific length and sequence. Traditionally, the purification of RNA transcripts is achieved by preparative denaturing (8 M urea) PAGE and subsequent electroelution from the polyacrylamide gel matrix *(34)*. This method separates large quantities of the desired RNA from unincorporated nucleotides and short, abortive transcripts with single nucleotide resolution, but tends to be laborious and time consuming. Additional disadvantages are the co-purification of water-soluble acrylamide impurities that are a result of incomplete polymerization along with the RNA transcript. These impurities show a high affinity for RNA, and their complete removal by dialysis is difficult, necessitating either additional purification steps or extensive rinsing of the RNA transcript with water using an appropriate CentriPrep concentrator.

An alternative purification protocol employs anion-exchange chromatography *(35, 36)*. Using this fast chromatography purification approach, the most time-consuming step for preparing large quantities of RNA for structural studies – PAGE purification followed by electroelution – can be eliminated and sample contamination with acrylamide is circumvented. It should be noted that this technique also preserves the co-transcriptionally adopted folding state of the desired RNA. This is in marked contrast to denaturing PAGE purification, which is typically accompanied by several precipitation steps, and represents an important advantage in cases in which annealing procedures fail to reproduce a natively folded RNA target.

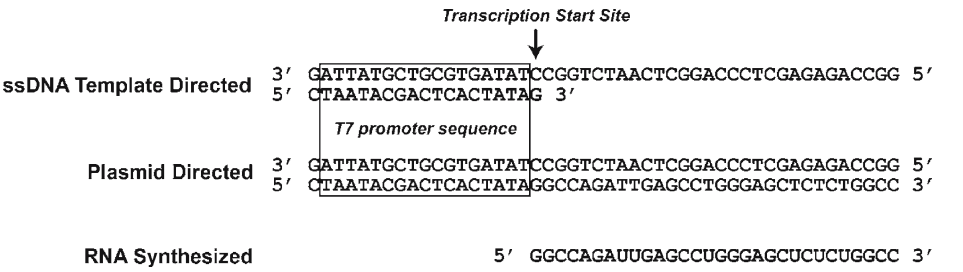

Fig. 2.4. Single and double-stranded DNA template sequences for the *in vitro* transcription of the HIV-2 TAR RNA (*see* **Note 2**).

3.1.1. Large-Scale DNA Template Directed In Vitro RNA Transcription

1. Transcription reactions are carried out under the following conditions: 80 mM K-HEPES (pH 8.1), 1 mM spermidine, 10 mM DTT, 0.01% Triton X-100, 80 mg/mL PEG-8000, 8–48 mM $MgCl_2$, 2–6 mM each NTP, 0.3 µM template oligonucleotide DNA, 0.3 µM promoter oligonucleotide DNA, and ~2,000–4,000 units/mL T7 RNA polymerase (*see* **Notes 11, 12,** and **13**).
2. The reactions are incubated for 4 hours in a water bath at 37°C.
3. The reactions are quenched with the addition of 0.1 volume of 0.5 M EDTA (pH 8.0) (*see* **Note 14**).
4. The reactions are extracted with an equal volume of phenol/chloroform (1:1, v/v) equilibrated with TE buffer to remove T7 RNA polymerase prior to purification. The organic layer is further extracted with an equal volume of water to ensure all the RNA is removed from the reaction.
5. The aqueous layers are combined and back extracted with an equal volume of chloroform/*i*-amyl alcohol (29:1, v/v) to remove any traces of phenol.
6. The aqueous layer is ethanol precipitated with the addition of 0.1 vol of 3 M sodium acetate and 3.5 volumes cold 100% ethanol at –20°C.
7. The crude RNA precipitate is collected by centrifugation, and resuspended in equal volumes of 80% Formamide Stop/Loading Buffer and 8M urea.
8. The sample is suitable for loading to a denaturing polyacrylamide gel.

3.1.2. RNA Purification by Denaturing Polyacrylamide Electrophoresis

1. These instructions are general and are easily adaptable to other formats, and reaction scales, including minigels. It is critical that the glass plates for the gels are extensively cleaned with detergent (e.g., Alconox, Alconox, New York, NY), ammonium-based glass cleaner (e.g., Wendex, S.C. Johnson), and finally 95% ethanol.
2. Prepare a polyacrylamide gel of the appropriate percentage, size, and thickness by mixing acrylamide/bisacrylamide solution, 1 µL APS and 1 µL TEMED per mL acrylamide/bisacrylamide solution *(32)*. The gel should polymerize in about 30 minutes.
3. Once the gel polymerizes, carefully remove the comb and wash the wells with TBE running buffer.
4. Place the gel into the appropriate gel running apparatus and add TBE running buffer to the upper and lower chambers of the gel unit.

5. Complete the assembly of the gel unit by connecting the power supply. The gel should be pre-run for at least 30 minutes at the appropriate voltage to allow thermal equilibration of the gel plates, prior to loading your samples.
6. Run the RNA sample a sufficient time to resolve the *n-1* nucleotide transcription product, typically two-thirds of the gel if the correct percentage polyacrylamide gel was used.
7. Take the gel off the apparatus and carefully remove the gel from the plates, placing the gel on clear cellophane.
8. The RNA can be easily visualized by UV_{256} shadowing, and excised from the gel with a clean razor blade or scalpel.
9. Place the gel pieces into an Elutrap Electroelution System in TBE running buffer at 4°C, and the RNA is extracted from the gel in a manner outlined by the vendor. Typically, removing four fractions over a period of 6 hours at 200V is sufficient to extract RNA from even a twenty percent polyacrylamide gel.
10. The RNA containing fractions are combined and precipitated by adding one-tenth the volume of 3M sodium acetate, followed by 3.5 volumes of cold 100% ethanol. Place the solution at –20°C.
11. The desired RNA is collected by centrifugation.
12. RNA samples are desalted using an appropriate CentriPrep concentrator and lyophilized.
13. The lyophilized RNA is dissolved in desired final volume (e.g., 500 µL for a standard 5-mm NMR sample tube) of NMR buffer.
14. The NMR sample is annealed in a manner appropriate to the specific RNA to form native structure (*see* **Note 15**).

3.1.3. RNA Purification by Anion-Exchange Chromatography

1. The transcription reaction is clarified by centrifugation (14,000*g*) to remove traces of precipitated pyrophosphate (*see* **Note 16**).
2. Equilibrate two HiTrap Q columns (Amersham Pharmacia) in low salt loading buffer at room temperature.
3. The transcription reaction mixture is applied to the equilibrated columns.
4. To separate the desired RNA from unincorporated nucleotides and plasmid DNA template, the loaded sample is typically eluted at a low flow rate of 1 mL/minute, in 3-mL fractions, with an increasing KCl gradient created by simultaneously decreasing the percentage of low salt loading buffer and increasing the percentage of high salt elution buffer being passed through the columns.

5. A common gradient for anion-exchange purification after transcription starts with 100% loading buffer to wash the columns, continues through a gradual climb from 0% to 60% elution buffer for the first 2 hours, then to 100% elution buffer over another 5 minutes. A typical elution profile, detected at 260 nm, generally shows three major peaks: the first one containing unincorporated nucleotides and short, abortive transcripts; the second peak containing the desired RNA; and the last fractions containing the plasmid DNA template (*see* **Note 17**).
6. Pure fractions are combined and concentrated using an appropriate CentriPrep (Millipore) concentrator.
7. Concentrated fractions are desalted and buffer exchanged by passage through a NAP25 gel filtration column (Amersham Pharmacia) equilibrated with an NMR buffer. Alternatively, pure fractions can also be dialyzed into NMR buffer, and then concentrated with a CentriPrep concentrator.
8. NMR samples are concentrated to desired final volumes (e.g., 500 µL for a standard 5-mm NMR sample tube) using an appropriate CentriPrep concentrator.

3.2. NMR Resonance Assignment and Restraint Collection

3.2.1. Resonance Assignment Strategy

Assignment of RNA resonances is commonly achieved through identification of sequential base to ribose nuclear Overhauser effect (NOE) patterns seen in helical regions of nucleic acid structure (**Fig. 2.5**), in analogy to the procedure originally utilized for DNA studies in the 1980s *(37)*. With the advent of isotopic labeling for RNA, the basic NOE assignment approach was initially expanded to include multi-dimensional (3D and 4D) versions of the standard nuclear Overhauser effect spectroscopy (NOESY), which simplified assignment and identification of NOEs *(38, 39)*.

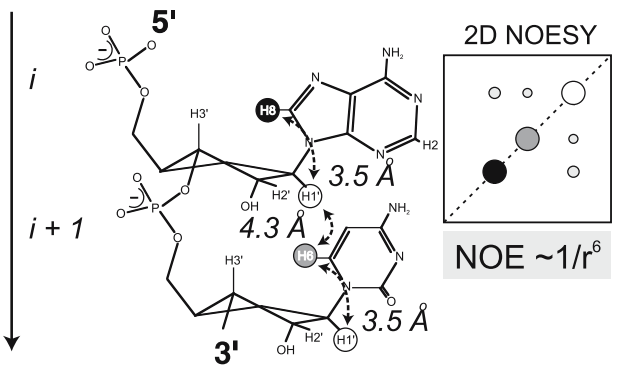

Fig. 2.5. Schematic representation of a 5′-pApC-3′ dinucleotide with arrows indicating the intra- and interresidual distances used for NOE based sequential assignments of A-form helical conformations. A schematic 2D NOESY with cross-peaks correlating H1′(i)- H8(i), H1′(i)-H6(i+1), and H1′ (i+1)-H6(i+1) is shown.

The NOE-based approach, however, relies on assumptions about structure and assignments, and is susceptible to errors from structural bias; methodology that achieves sequential assignment via unambiguous through-bond correlation experiments, as is the case for proteins, would be more ideal. Unfortunately, complete sequential assignments of even medium-sized RNA molecules using through-bond experiments such as HCP (*see* **Note 18**), HCP-TOCSY (*To*tal *C*orrelation *S*pectroscop*y*) and HP-HETCOR (*Het*eronuclear *Cor*relation) are hampered by notoriously overlapped resonances and modest sensitivity. Thus, through-bond assignment using HCP-like experiments is not feasible for larger RNA target molecules (~20 kDa). A hybrid approach with HCN and NOESY experiments is the optimal compromise to achieve unambiguous assignments. The HCN experiments can determine intranucleotide correlations within and between the base and ribose resonances, which will significantly reduce the ambiguity present in the NOESY-based assignment procedure. HCCH-based experiments are used to unambiguously assign crowded ribose, pyrimidine H5/H6, and adenosine spin systems. A variety of through-bond correlation experiments facilitate the assignments of exchangeable imino- and amino proton resonances linked to non-exchangeable base H6 and H8 protons *(12, 40)*.

3.2.2. NMR Restraints for Structure Determination

After sequence-specific assignments of RNAs are obtained, the structure determination is based on collecting sufficient numbers of proton-proton distance restraints utilizing NOESY experiments. The structural analysis of the RNA backbone conformation is complicated by the lack of useful ^{1}H-^{1}H NOE distance restraints available that define the backbone torsions (**Fig. 2.6**).

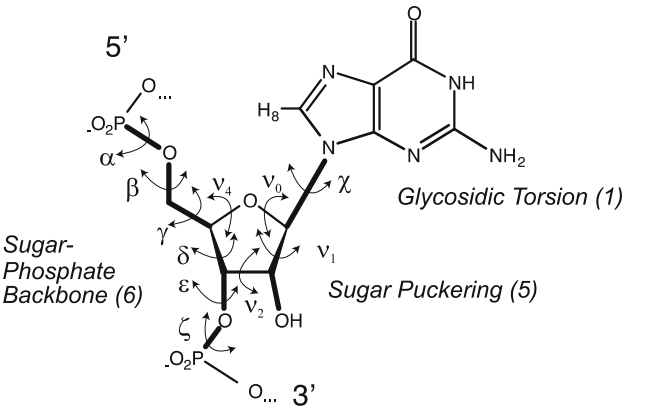

Fig. 2.6. Schematic representation of a 5′-pGp-3′ mononucleotide with arrows indicating the various torsional degrees of freedom in the sugar-phosphate backbone, the pentose ring, and the glycosidic torsion.

Potentially, the short distance restraints between pairs of protons (<6Å) can be complemented with torsion angle information accessible through J-coupling constants. Vicinal ^3J scalar coupling constants can provide useful structural information about the sugar pucker, the β and ε backbone torsion angle conformations, as well as the glycosidic torsion χ, which defines the orientation of nucleobases with respect to the sugar moiety. In addition, NMR experiments have been introduced that allow the direct identification of donor and acceptor nitrogen atoms involved in hydrogen bonds. These recently introduced parameters are especially important for structure determination of RNA due to the low proton density.

However, there is a practical difficulty in defining RNA structures precisely by NMR because NOE and J-coupling–based structure calculation relies on either short range distance (<6Å) or local torsion angle information. RNAs often are elongated structures, which are better approximated as cylindrical rather than globular shapes. There is a lack of NOE information between distant ends of the molecule; as a result, the relative orientations of helical segments at opposite ends of the molecule are poorly defined. Recent advances in methodology help to alleviate or overcome this shortcoming *(15, 41)*.

New experiments to measure orientational, rather than distance-dependent, dipolar couplings and cross-correlated relaxation rates have been developed, providing additional structural information. Methods have been developed to create a slightly anisotropic environment for molecules tumbling in solution. This results in a small degree of alignment of the molecule, and the dipolar couplings no longer average to zero, while retaining the quality of high-resolution NMR spectra. The most promising system for NMR studies of partially aligned RNA is a Pf1 bacteriophage solution *(16, 42)*. There is a narrow useful range of alignments suitable for high-resolution NMR studies. Higher phage concentrations are associated with stronger alignments and produce larger residual dipolar couplings, whereas lower concentrations correspond to lower degrees of ordering, reflected in smaller dipolar couplings. Too much alignment gives larger dipolar couplings, but also results in line broadening to such an extent that high-resolution NMR is not possible.

Residual dipolar couplings (RDC) data should be combined with the traditionally used NOE distance restraints and torsion angles derived from scalar J-couplings. The RDC data do not only provide additional information for a better definition of the global orientation of the three stems with respect to each other, but also carry valuable information on the dynamic properties of the RNA studied *(43–45)*.

3.2.3. NOE Distance Restraints

1. The main source of structural data will still be obtained from NOEs, which provide distance restraints for pairs of hydrogen atoms. Only short proton-proton distances in the range <6Å are accessible through NOESY-type experiments. Identification of NOEs will be facilitated by resolving the ^{1}H,^{1}H NOE connectivities that are essential for determining the structure into three and four dimensions through detection of the heteronuclear (^{13}C/^{15}N) chemical shifts of the proton-attached nuclei.
2. NOESY-type experiments should be recorded with varying mixing times (50–300 ms). NOE cross peaks obtained with long mixing times (>100 ms) are harder to quantitate and should be used with caution in structure calculations; however, they can tremendously help during the assignment process (*see* **Notes 19, 20, 21,** and **22**).
3. Imino proton resonances should be assigned sequence specifically at an early stage from water flip-back, WATERGATE-2D NOESY *(46)* spectra (τ_{mix} = 200 ms) to verify the construct integrity and secondary structure predictions (**Fig. 2.7**).
4. The identification of NOEs can be further facilitated by utilizing isotope filtered/edited NOESY experiments in combination with nucleotide-specific isotopically labeled RNA *(47)*.

3.2.4. Torsion Angle Restraints

1. The ribose sugar geometry is defined by five alternating torsion angles (ν_0 through ν_4). Usually, the ribose sugar adopts one of the energetically preferred C2′-endo (South) or C3′-endo (North) conformations. A number of ^{1}H,^{1}H and ^{1}H,^{13}C scalar couplings are available to determine the sugar pucker

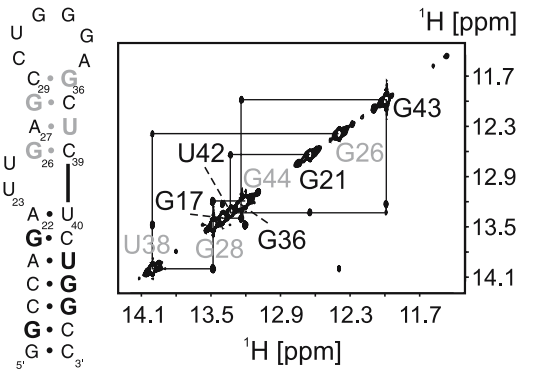

Fig. 2.7. 2D ^{1}H,^{1}H water flip-back, WATERGATE NOESY *(46)* spectrum of the TAR RNA (τ_{mix} = 200 ms). Sequential assignments of the imino proton resonances by NOE connectivities are indicated. The observable upper stem G and U residues are shown in bold gray and lower stem G and U residues in bold black.

qualitatively with the combination of H1′-H2′ and H3′-H4′ coupling constants being the most useful for smaller RNAs. The ^{3}J(H1′,H2′) vicinal coupling is >8 Hz for C2′-endo puckers and ~1 Hz for C3′-endo puckers (**Fig. 2.8**), typically found in A-form helices *(48–50)*. The opposite behavior is expected for the ^{3}J(H3′,H4′) coupling constant with C2′-endo puckers associated with small and C3′-endo puckers with relatively large coupling constant values (*see* **Note 23**).

2. Measurement of the γ torsion is difficult due to the need for stereospecific assignments of the H5′ and H5′ proton resonances. The two-bond C4′,H5′/H5″ couplings can be used in conjunction with the vicinal H4′,H5′/H5″ couplings to define γ *(50, 51)*.
3. Two heteronuclear vicinal ^{1}H,^{13}C couplings contain useful information about the glycosidic torsion angle χ. The ^{3}J(H1′,C) couplings involving the C4,C8 carbons in purines and the C2,C6 carbons in pyrimidines, respectively, all depend on the χ torsion *(50, 52)*. The preferred orientation around χ in A-form helix is *anti*, which makes the base accessible for commonly found hydrogen bonding interaction.
4. The ε and β torsions can be determined by measuring a variety of ^{13}C,^{31}P and ^{1}H,^{31}P scalar couplings. Some of these torsions may be measured directly in 2D ^{1}H,^{31}P heteronuclear COSY (or HETCOR) experiments *(53, 54)* and non-refocused ^{1}H,^{31}P

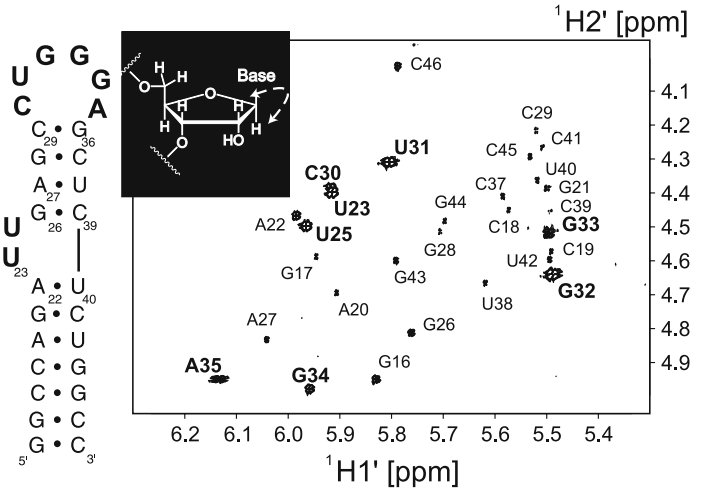

Fig. 2.8. Ribose H1′-H2′ region of a 2D ^{1}H,^{1}H DQF (*Double Quantum Filtered*): COSY *(129)* spectrum of the TAR RNA. Assignments for the H1′-H2′ cross-peaks probing the individual sugar puckers are indicated. Residues shown in bold adopt either C2′-endo or mixed C2′-endo/C3′-endo sugar puckers, resulting in more efficient magnetization transfer due to larger ^{3}J(H1′,H2′) couplings. Weaker cross-peaks are associated with residues adopting C3′-endo sugar puckers, typically found in A-form helices. The inset shows a ribose ring; the arrow highlights the H1′- H2′ connection.

HSQCs (*H*eteronuclear *S*ingle *Q*uantum *C*oherences) if the phosphorus and proton resonances are sufficiently resolved (**Fig. 2.9**). However, both the ribose proton and phosphorus resonances involved are generally overlapped for even moderate size RNAs. Accurate measurements for $^{13}C,^{31}P$ and $^{1}H,^{31}P$ couplings can be obtained from both phosphorus-fitting of doublets from singlets (so-called P-FIDS) *(55)* or spin echo difference experiments (56–60). J-HMBC techniques can be applied to determine $^{3}J(H,P)$ couplings *(61)*. A quantitative version of the HCP experiment allows for quantitation of $^{3}J(C4',P)$ *(62)*.

5. The α and ζ torsions are not accessible by J-coupling measurements because the involved ^{16}O nuclei have no magnetic moment. Some groups have used ^{31}P chemical shifts as a guide for loose constraints on these torsions *(63)*; however, the correlation between ^{31}P chemical shifts and the phosphodiester backbone conformation is not well understood in RNA.
6. Cross-correlated relaxation rates have been introduced to high-resolution NMR as a novel parameter for structure determination *(18, 19)*. Such methods have been employed to gain information on the α and ζ torsions. The cross-correlated relaxation between a ribose ^{13}C-^{1}H dipole and the ^{31}P chemical shift anisotropy (CSA) carries valuable structural information about the phosphodiester conformation *(64)*. Additionally, applications have been published where the cross-correlated relaxation between a ^{13}C-^{1}H dipole

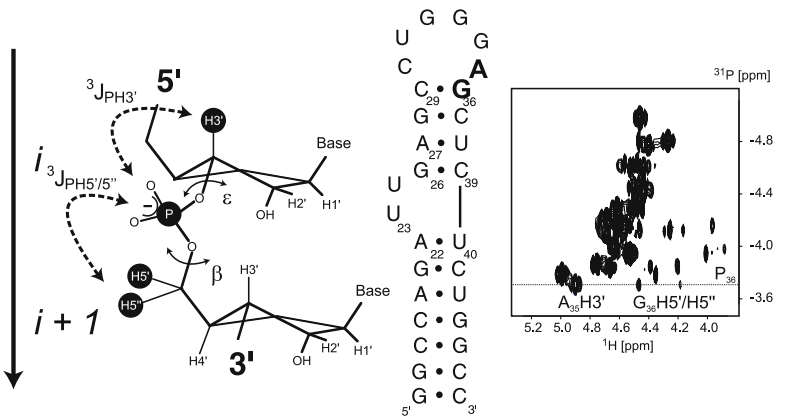

Fig. 2.9. Schematic representation of a 5′-NpN-3′ dinucleotide with arrows highlighting the $^{3}J(H3',P)$ and $^{3}J(H5'/5'',P)$ couplings associated with the torsion angles ε and β, respectively. 2D $^{1}H,^{31}P$-HETCOR spectrum of the TAR RNA *(53)*. Assignments for the H3′/H5′/H5″,^{31}P-correlations along the $^{31}P36$ resonance are indicated in the spectrum and shown in bold in the secondary structure representation.

and the glycosidic ^{15}N CSA is utilized to collect information about the glycosidic torsion angle χ *(65, 66)*. Another example is the measurement of cross-correlated relaxation rates between neighboring ^{13}C-^{1}H dipoles within the ribose ring that can be used to define the sugar pucker. For RNAs, cross-correlated relaxation rates can be measured using an experiment that belongs to the HCCH class, and precisely determine the ribose sugar pucker without the need of any empirical Karplus parameterization *(67)*. The resolution of this experiment can be further enhanced by a combination with a CC-TOCSY transfer *(68)* (*see* **Note 24**).

3.2.5. Residual Dipolar Coupling Restraints

1. One-bond dipolar couplings on the order of ±10–30 Hz can be introduced using ~15 mg/mL filamentous Pf1-phages as co-solutes, which creates an anisotropic environment for the RNA target molecule (*see* **Note 25**).
2. For a directly bonded pair of nuclei with known distance, such as ^{1}H-^{13}C or ^{1}H-^{15}N in labeled RNA, angular restraints can be extracted from dipolar coupling data and incorporated during the structure calculation. Such one-bond dipolar couplings can be measured in a straightforward and sensitive manner. The difference between scalar J coupling constant values measured in isotropic and anisotropic media gives the residual dipolar coupling. Two NMR experiments are commonly performed to measure one bond ^{1}D(H,C) RDC constants. Base C2-H2, C5-H5, C6-H6, and C8-H8 dipolar couplings are typically derived from analyzing peak positions in CT-TROSY and CT-antiTROSY experiments *(69)*. For the ribose 1′–4′ one-bond dipolar couplings, a J-modulated CT-HSQC should be acquired *(70)*. A J-modulated ^{1}H,^{15}N-HSQC provides additional one bond ^{1}D(H,N) RDC restraints *(71)*.
3. The determination of the phosphate backbone conformation in solution remains an experimentally intriguing problem. New parameters based on incomplete averaging in partially aligned RNA samples such as dipolar ^{1}H,^{31}P couplings *(53, 72, 73)* or ^{31}P CSA *(74)* hold the promise to significantly impact on the precision of RNA structure determination in solution.

3.2.6. Hydrogen Bond Restraints

1. Canonical base-pair hydrogen bonding of the Watson-Crick type is fundamental in all biological processes in which nucleic acids are involved. The partially covalent character of hydrogen bonds gives rise to measurable scalar spin-spin couplings of, for example, the type ^{h2}J(N,N) and ^{h1}J(H,N) that represent important additional NMR parameters for the structure determination of nucleic acids in solution *(20, 21)*. In addition to the unambiguous determination of donor D

and acceptor A nuclei involved in hydrogen bond formation, the magnitude of the $^{h}J(D,A)$ couplings reports on the hydrogen bond geometry and could potentially provide more precise distance information for structure calculations. The simultaneous identification of nuclei involved in hydrogen bonds and quantification of corresponding $^{h2}J(N,N)$ scalar couplings is accomplished using a HNN-COSY (*Co*rrelation *S*pectroscop*y*) experiment or one of its variants (**Fig. 2.10**).

2. Several groups have also reported measuring scalar couplings across hydrogen bonds in non-canonical base pairs and in tertiary structural interactions *(75–81)*.
3. The large two-bond $^{2}J(H,N)$ scalar couplings within the purine bases allow reasonably efficient magnetization transfer during INEPT (*I*nsensitive *N*uclei *E*nhancement by *P*olarization *T*ransfer) delays *(82)*. The independent assignments of potential nitrogen hydrogen bond acceptor sites using the intra-residue $^{2}J(H2,N1)$, $^{2}J(H2,N3)$, and $^{2}J(H8,N7)$ correlations for the purine residues in the RNA molecule can be obtained from a two-bond $^{2}J(H,N)$ $^{1}H,^{15}N$-HSQC experiment.
4. The 2′-hydroxyl group plays fundamental roles in both the structure and function of RNA and is the major determinant of the conformational and thermodynamic differences

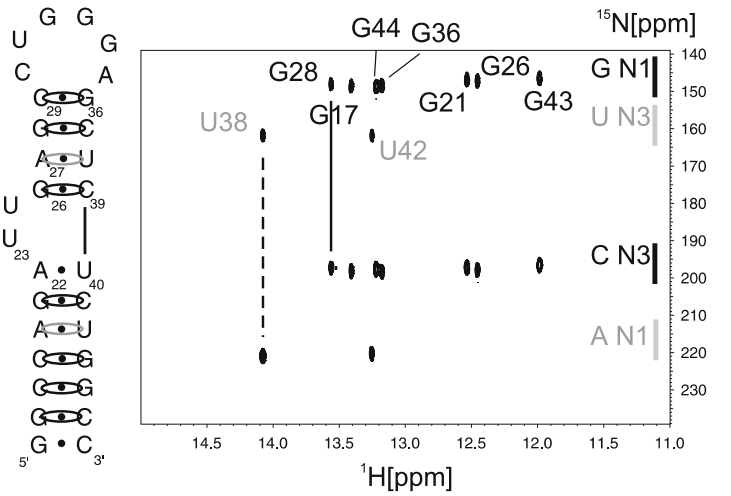

Fig. 2.10. 2D $^{1}H,^{15}N$ HNN-COSY of the TAR RNA. Assignments of the imino proton nitrogen correlations are indicated with the observable G and U residues shown in black and gray, respectively. Canonical base-pair hydrogen bonding of the Watson-Crick type correlates U N3 nitrogen donor sites with A N1 nitrogen acceptor sites (dashed line) and G N1 nitrogen donor sites with C N3 nitrogen acceptor sites (solid line). Typical ^{15}N chemical shift ranges are indicated; solid black bars highlight G N1 and C N3 nitrogens, while gray bars highlight A N1 and U N3 nitrogen chemical shift ranges.

between RNA and DNA. In aqueous solution the rapid exchange of the hydroxyl proton with the solvent typically prevents its observation in RNA at room temperature by NMR. Most recently, a conformational analysis of 2′-OH hydroxyl groups of the HIV-2 TAR RNA by means of NMR scalar coupling measurements in solution at low temperature has been reported *(83, 84)*. Cross hydrogen bond scalar couplings involving two slowly exchanging 2′-OH hydroxyl protons were observed and analyzed in a frame shifting mRNA pseudoknot *(85)*.

3.2.7. Base-to-Base H(C/N)H-Type Correlation Experiments

1. A set of HNCCH- and HCCNH-TOCSY experiments have been developed that correlate the exchangeable imino and amino proton resonances with the non-exchangeable base resonances for the complicated spin systems of all four nucleotides as shown in **Fig. 2.11** *(81, 86–91)*.
2. Complementary HCCH-COSY *(92)* and HCCH-TOCSY *(93, 94)* experiments are used to unambiguously assign pyrimidine H5/H6 and adenosine spin systems.

3.2.8. Base-to-Ribose HCN-Type Correlation Experiments

1. Optimized HCN-type pulse schemes for the through-bond correlation of ribose and base resonances utilizing MQ (multi-quantum)- instead of SQ (single-quantum)-evolution periods have been proposed and show significant sensitivity gains, essential for successful investigations of larger RNA systems *(95, 96)*. Also, TROSY (*T*ransverse *R*elaxation-*O*ptimized *S*pectroscopy) versions of HCN experiments have been successfully applied to RNA *(97, 98)*.

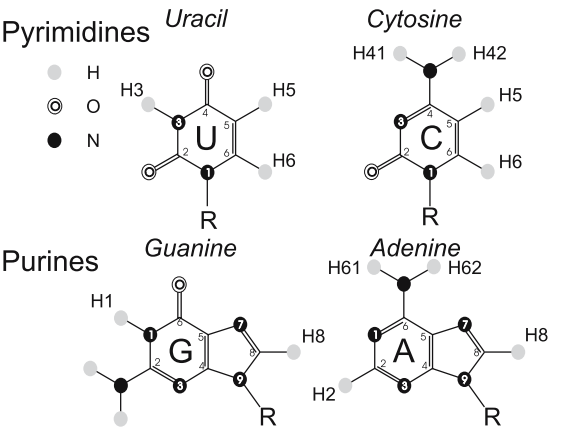

Fig. 2.11. The four different aromatic nucleobases, uracil, cytosine, guanine, and adenine. Exchangeable imino and amino proton resonances and non-exchangeable aromatic proton resonances that are correlated in HNCCH- and HCCNH-TOCSY experiments are shown as gray circles.

2. In favorable cases, magnetization can be transferred all the way through from the anomeric H1′ proton to the base H6/8 protons circumventing assignments through joint glycosidic N1/9 nitrogen chemical shift *(99, 100)*.

3.2.9. Ribose-to-Ribose HCCH-Type Correlation Experiments

1. The magnetization transfer through the ribose proton spin systems is hampered due to the small $^{3}J(H1',H2')$ vicinal coupling, present in most commonly populated A-form RNA, correlating the H1′ and H2′ resonances. Ribose proton spin system assignments from homonuclear ^{1}H, ^{1}H -COSY- and TOCSY experiments can be obtained more readily using HCCH-COSY and -TOCSY experiments on ribose rings uniformly labeled with ^{13}C, which allows magnetization transfer and chemical shift evolution on the C1′ to C5′ carbons *(39, 101–104)*.
2. The powerful hybrid HCCH-COSY-TOCSY *(105, 106)* experiment can also be employed to unambiguously assign crowded ribose spin systems.

3.2.10. Ribose-to-Phosphate Backbone H(C)P-Type Correlation Experiments

1. For unlabeled RNAs, a number of relatively efficient ^{1}H,^{31}P-multi-dimensional correlation schemes are available for sequential assignment of ^{31}P and ribose ^{1}H resonances. Magnetization can be transferred from excited ^{31}P resonances to the $^{3}J(H,P)$ scalar coupled ribose protons for detection using either COSY- *(54)* or heteronuclear TOCSY-type *(107)* transfer steps. The resulting two-dimensional H3′/H5′/H5″,^{31}P-correlations can be concatenated with homonuclear ^{1}H,^{1}H NOESY or TOCSY experiments to transfer magnetization to potentially better resolved resonances like H1′ or aromatic H8/H6 resonances *(108, 109)*.
2. A straightforward extend approach for ^{13}C labeled RNAs is HCP correlation via sequential INEPT transfers ($^{1}H \rightarrow {}^{13}C \rightarrow {}^{31}P \rightarrow {}^{13}C \rightarrow {}^{1}H$) *(110, 111)* correlating nuclei of adjacent nucleotides i and i + 1 (**Fig. 2.12**). Subsequent experiments, HCP-CCH-TOCSY (112) and P(CC)H-TOCSY *(113)* combine the HCP and HCCH-TOCSY experiments and thus resolve relevant correlations on the better dispersed C1′/H1′ resonances.

3.3. Structure Calculation

3.3.1. Generation of Restraint File

1. The intensity of NOESY cross peaks is approximately proportional to the inverse of the averaged distance to the power of six, $\langle 1/r_{ij}^{6} \rangle$, assuming an isolated pair of proton spins i and j. For RNA NMR studies, NOE-derived distance restraints are often determined semi-quantitatively and placed into four categories: strong, medium, weak, and very weak NOEs. A conservative approach sets all the lower bounds to 1.8 Å

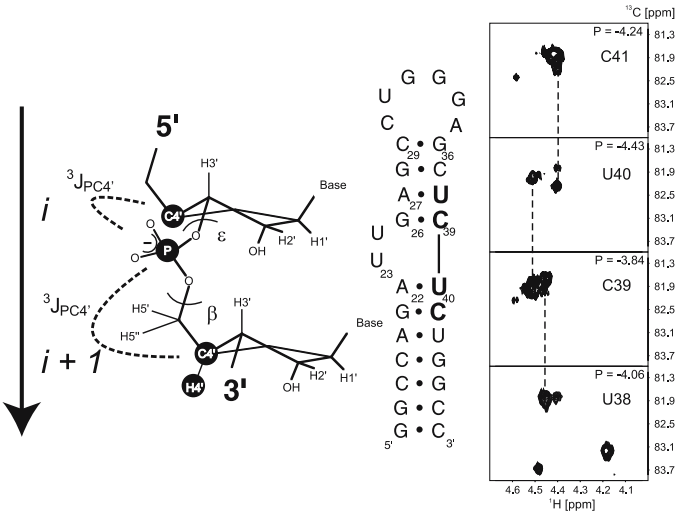

Fig. 2.12. Schematic representation of a 5′-NpN-3′ dinucleotide with arrows highlighting the ^{3}J(C4′,P) couplings associated with the torsion angles ε and β, respectively. 2D ^{1}H4′,^{13}C4′ planes of a 3D HCP spectrum of the TAR RNA. Sequential assignments for the ^{1}H4′,^{13}C4′-correlations along the ^{31}P resonance frequencies of C41, U40, C39, and U38 are indicated (dashed lines) and shown in bold in the secondary structure representation.

(van der Waals radius) with upper bounds ranging from 3.0 Å for the most intense NOEs to 7.0 Å for the weakest NOEs found in H_2O experiments.
CNS/Xplor syntax as compiled in distance restraint table (e.g., noe.tbl):

assign <1st atom-sel.> <2nd atom-sel.> <distance> <d_{minus}> <d_{plus}>

Example: proton H1 of residue 4 and proton H4′ of residue 30 are separated by 2.4 ± 0.6 Å

assign (resid 4 and name H1) (resid 30 and name H4′) 2.4 0.6 0.6

2. J-coupling restraints can be implemented in two different ways during the structure determination. They can be introduced qualitatively by restricting a torsion angle in a loose manner (±30°) to one of the three staggered rotamers along the phosphodiester backbone, or defining the preferred ribose sugar pucker such as C2′-endo or C3′-endo. Alternatively, vicinal J-couplings can be quantitatively related to a certain torsion angle using semi-empirical Karplus relations of the form: $^{3}J = A\cos^{2}\theta + B\cos\theta + C$, where θ is the intervening torsion angle *(40, 114)*.
CNS/Xplor syntax as compiled in torsion angle restraint table (e.g. torsion.tbl):

assign <1st atom-sel.> <2nd atom-sel.>
<3rd atom-sel.> <4th atom-sel.> <real> <real> <real> <integer>

The four numbers are, respectively:

1. Force constant in kcal/(mole radians exp{exponent})
2. Equilibrium torsion angle in degrees
3. Range around the equilibrium value in degrees
4. Exponent for restraint calculation

Example: restrict residue 2 to North or C3′-endo sugar pucker

```
The sugar pucker can be defined with the
following ribose torsion angles: ν1 = O4′-
C1′-C2′-C3′ and ν2 = C1′-C2′-C3′-C4′.
assign (resid 2 and name O4′) (resid 2 and
name C1′)
     (resid 2 and name C2′) (resid 2 and
     name C3′)
     1.0–20.0 10.0 2
assign (resid 2 and name C1′) (resid 2 and
name C2′)
     (resid 2 and name C3′) (resid 2 and
     name C4′) 1.0 35.0 5.0 2
```

3. The size of dipolar couplings for an axially symmetric RNA molecule depends on the average value of an orientational function, $\frac{1}{2}(3\cos^2\theta - 1)$, and the inverse cubic distance, $1/r^3$, between the coupled nuclei. Here, the angle θ characterizes the axial orientation of the internuclear vector that connects the coupled nuclei with respect to the principal axis system of the molecular alignment tensor.

```
CNS/Xplor syntax as compiled in RDC table
(e.g., dipolar.tbl):
A pseudomolecule OXYZ is defined with orthogo-
nal vectors OX, OY, and OZ. OXYZ reorients it-
self during the refinement process to satisfy
the experimentally measured RDC data against
an energy penalty with its origin fixed in
space away from the target RNA molecule.
assign <external origin-sel.>
     <z-unit vector-sel.>
     <x-unit vector-sel.>
     <y-unit vector-sel.>
     <1st atom-sel.> <2nd atom-sel.> <RDC>
     <RDC_error>
Example: An RDC value of 15.6 ± 0.6Hz is
measured for the one-bond interaction bet-
ween C1′ and H1′ of residue 2:
assign (resid 500 and name OO)
     (resid 500 and name Z)
     (resid 500 and name X)
     (resid 500 and name Y)
     (resid 2 and name C1′)
     (resid 2 and name H1′) 15.6000 0.6000
```

3.3.2. Molecular Dynamics Simulation

1. Most commonly, starting structures are calculated from randomized RNA coordinates using solely energy terms from holonomic constraints such as geometric and non-bonded terms using restrained molecular dynamics calculations.
2. To generate a family of structures consistent with the NMR data, the second step refines against the experimentally derived NOE distance and torsion restraints. We typically follow widely used approaches using restrained molecular dynamics in torsion angle space. Families of structures are generated from random extended structures in Xplor *(115)* or CNS *(116)* using *ab initio* simulated annealing. Torsion angle dynamics (TAD) as implemented into, e.g., Xplor or CNS proved to be robust and have a higher convergence rate with respect to molecular dynamics in Cartesian coordinate space *(117)*.
3. The generated structures are further refined against RDC data in a series of molecular dynamic runs with increasing dipolar force constants. Xplor and CNS provide modules for refinements against novel NMR parameters, for example, chemical shifts and anisotropic interactions such as RDCs and phosphorus chemical shift anisotropies.
4. The lowest energy structures after simulated annealing and subsequent refinement against sets of RDCs collected are minimized using the AMBER module Sander *(118)*. Due to more adapted force fields, AMBER yields better and more consistent results for nucleic acids *(119)*.

3.3.3. Structural Statistics

1. In evaluating the quality of a family of RNA NMR structures, a number of statistics can be evaluated: Root Mean Square Deviation (RMSD), number of NOE, RDC, and torsion restraints; residual distance, dipolar coupling, and torsion violations; and the largest distance, dipolar coupling, and torsion violations. Typically, the distance restraints are further dissected into the number of inter-residue, intra-residue, and inter-molecular NOEs.
2. Useful RMSDs to consider include only regions of interest and are usually a more accurate descriptor of the quality of the structure than the overall global RMSD. Local RMSDs are given because the overall global RMSD can easily be in the 2.0–3.0 Å range, which might otherwise be indicative of poor convergence. Almost every RNA structure studied includes a region that is poorly defined, such as a disordered loop, terminal base pair, or a nucleotide without any inter-nucleotide NOEs. This situation is comparable to protein NMR studies, which often neglect the N and C terminal ends of proteins because of the lack of structural data from these regions (*see* **Note 26**).

3. In contrast to crystallographic B-factors, a general measure for the uncertainty in NMR-derived structures is not available. The commonly used RMSD, which is a measure for the precision of the data, tends to overestimate the accuracy of NMR structure ensembles and therefore is a problematic measure for the uncertainty in the atomic coordinates. However, the measurement of a large set of RDCs permits cross-validation to assess the accuracy of NMR-derived atomic coordinates. Structure calculations should be carried out omitting a randomly chosen subset of the RDC data while refining against the remaining RDCs. The accuracy of a family of RNA NMR structures is cross-validated by the agreement between the structures (which are used to back-calculate the RDCs) and the omitted RDC subset *(120, 121)*. Alternatively, a comparison between calculated and observed ^{1}H chemical shifts represents another possibility for cross-validation of structures derived from NMR restraints *(122)*.

4. Notes

1. Unless stated otherwise, all solutions should be prepared in water that has a resistivity of 18.2 MΩ•cm and total organic content of less than five parts per billion. This standard is referred to as "water" in the text.
2. The T7 promoter DNA strand used for oligonucleotide-based *in vitro* transcription should be of the following sequence: 5′-C TAA TAC GAC TCA CTA TAG-3′. The addition of a cytidine nucleotide 5′ of the T7 promoter sequence increases stability of the dsDNA and increases yields of product RNA *(123)*.
3. When designing the template strand of ssDNA, care should be taken at both the 5′, as well as 3′ end to insure optimal yields of RNA *(3, 4)*. If the RNA product contains unacceptable 3′-end inhomogeneity, the template ssDNA can be prepared with a 5′ non-hydrogen bonding nucleoside such as 4-methylindole *(124)*. Alternatively, the desired RNA can be transcribed with a 3′-end flanking sequence that folds into a hammerhead ribozyme that cleaves co-transcriptionally to yield a homogenous 3′-end with a 2′-, 3′-cyclic phosphate group *(125, 126)*.
4. 5′-YpA-3′ steps in single-stranded regions constitute hot spots for RNA hydrolysis and thus can contribute to long-term chemical instability of an NMR sample. In favorable cases, these dinucleotide steps can be eliminated without compromising the RNA structure.

5. In addition to Notes 2, 3, and 4, care should also be taken when designing a restriction enzyme site at the 3′-end of the plasmid for linearization. The remaining nucleotides should not only reduce 3′-end inhomogeneity, but also should be compatible with secondary or tertiary interactions that may be present in the RNA.
6. It is recommended that nucleotide-5′-triphosphates should be prepared *(127)* or purchased (Sigma-Aldrich, St. Louis, MO; Cambridge Isotope Labs, Andover, MA) as the free acid, ammonium, or sodium salt whenever possible. In our hands, lower transcription yields can result when lithium, magnesium, triethylammonium, and cyclohexylammonium salts are used.
7. T7 RNA polymerase is commercially available (e.g., New England Biolabs, Beverly, MA) but expensive. We prepare T7 RNA polymerase for transcriptions from an *E. coli* overexpressing strain, several million Units at a time, approximately every 6 months.
8. Unpolymerized acrylamide/bisacrylamide is a neurotoxin; therefore, care should be taken to avoid direct exposure.
9. N,N,N,N-Tetramethyl-ethylenediamine (TEMED, Bio-Rad) is best stored at room temperature in a desiccator. Quality of gels and rate of polymerization decline after opening; therefore, purchasing small amounts of TEMED is recommended.
10. Ammonium persulfate (APS) is best stored at 4°C. Quality of gels and rate of polymerization decline over time; therefore, it is recommended that stocks should be prepared frequently.
11. If plasmid DNA is used, one should substitute for plasmid Transcription buffer and omit the PEG-8000.
12. During the transcription reaction, there is a buildup of pyrophosphate that may slow down and in extreme cases inhibit the polymerase reaction by sequestering Mg^{2+}. Transcription yields may be improved with the addition of 1 unit of inorganic pyrophosphatase (IPP, Sigma-Aldrich) per milliliter of transcription. IPP hydrolyzes (insoluble) pyrophosphates. Care should be taken to optimize the transcription in the presence of IPP.
13. Transcription yields may also be improved with the addition of 10 units of RNAase Inhibitor (RNAsin, Promega Corp.) per milliliter of transcription. Care should be taken to optimize the transcription in the presence of inhibitor.
14. When transcription optimizations are being performed, one can directly bring each reaction up in loading buffer and apply directly to the polyacrylamide gel.

15. No general procedures for annealing can be given as conditions can vary between RNAs. Typically, simple stem-loop structures such as the 30 nucleotide-containing TAR RNA can be properly annealed by heat denaturation (95°C for 2 minutes) followed by a snap-cooling step (4°C for 10 minutes) under low to moderate salt conditions.
16. Transcription reactions can be extracted with an equal volume of phenol/chloroform (Fisher Scientific) equilibrated with TE buffer (10 mM Tris-HCl, 1 mM EDTA, pH 8.0) to remove enzymes prior to anion-exchange chromatography.
17. Anion-exchange FPLC gradient conditions should be optimized to increase the resolution for each desired RNA target.
18. Names given to the through bond correlation experiments are derived from the series of nuclei through which magnetization is transferred during the experiment.
19. Before embarking on a detailed and time-consuming NMR investigation of a chosen RNA, it is extremely important to optimize the sample conditions for acquisition of the various required NMR experiments. It is critical to determine at the outset if the system is suitable for a high-resolution NMR structure elucidation. Considerations include: the RNA construct, salt concentrations, pH, and buffer type and concentration.
20. The imino proton region of the proton NMR spectrum of an unlabeled RNA sample in H_2O provides a sensitive diagnostic for this purpose. An example imino proton 1D spectrum for a correctly folded 30mer RNA is shown in **Fig. 2.13**. One peak should be observed for each Watson-Crick base pair in the molecule. Since the imino protons exchange

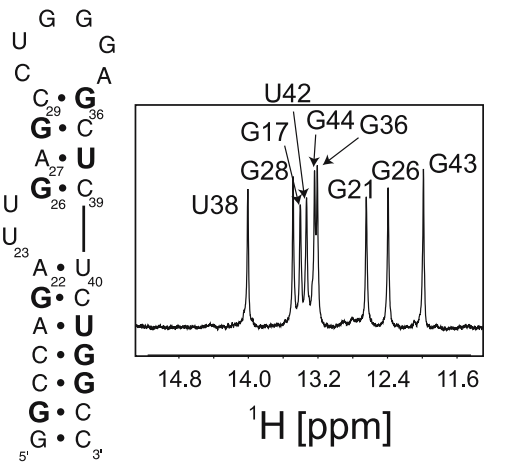

Fig. 2.13. 1D jump-return echo ^1H imino spectrum of the TAR RNA recorded in H_2O. Assignments for observable G and U imino protons are indicated and shown in bold in the secondary structure representation.

rapidly with the bulk H_2O, the spectrum was recorded with a jump-return echo sequence that avoids presaturation, while providing most efficient water suppression *(128)*. The pyrimidine base protons can provide a valuable alternative, circumventing problems related to solvent exchange. H5-H6 cross-peaks can be conveniently monitored in 2D TOCSY or COSY spectra; an example is given in **Fig. 2.14**.

21. The sample conditions are surveyed directly by NMR spectroscopy as a function of RNA and Mg^{2+} concentration in a phosphate buffer (10 mM Na- or K-phosphate, pH 6–7) with moderate monovalent salt (typically 50–100 mM NaCl or KCl) in order to identify constructs and solution conditions suitable for a subsequent structure determination. The goal is to obtain the narrowest line width and best chemical shift dispersion for the observable imino and/or H5-H6 base protons that report on secondary structure formation.

22. Potential problems with interpretation of obtained NOESY cross-peak intensities in terms of ^{1}H-^{1}H distances in structure calculations arise mainly from the phenomenon called spin diffusion. Spin diffusion causes a breakdown of the isolated spin pair approximation because other nearby protons provide competing indirect pathways for observing the direct NOE between the two protons. Spin diffusion effects play a role, especially when longer NOESY mixing times (>100 ms) are used. This usually leads to damped NOESY cross-peak intensities that build up through the direct pathway, resulting in underestimated interproton distances. Additionally, multistep transfer pathways can occur, resulting in false NOE assignments. For example, the imino protons of guanines might show spin diffusion mediated NOEs to the

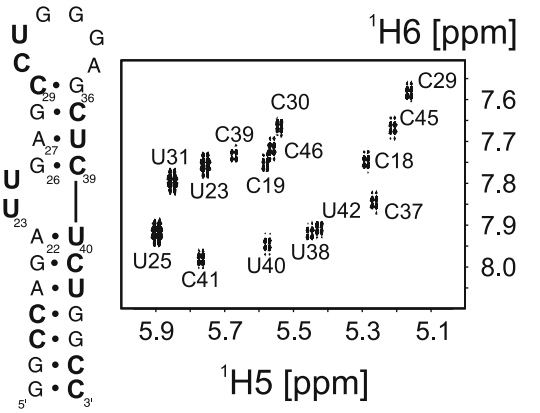

Fig. 2.14. H5-H6 region of a 2D ^{1}H,^{1}H DQF-COSY (129) spectrum of the TAR RNA. Assignments for the pyrimidine H5-H6 cross peaks are indicated and shown in bold in the secondary structure representation.

non-exchangeable aromatic H5 and H6 protons of cytidines in Watson-Crick base pairs through the cytidine amino protons. However, in an early stage of the assignment procedure based on NOESY correlations, spin diffusion pathways can aid the identification of spin systems. Thus, for assignments it is recommended to analyze NOESY spectra acquired with shorter (~50 ms) and longer (~150 ms) mixing times.

23. Often ribose puckers are found with homonuclear H1′,H2′/H3′,H4′ coupling constants in the 3–6 Hz, indicative of conformational exchange between the C2′- and C3′-endo puckers. This mixed conformation is typically left unrestrained.

24. The quantitative analysis of scalar J-couplings, especially in the case of homonuclear $^{3}J(H,H)$ couplings related to the ribose sugar pucker, becomes more and more difficult with increasing molecular weight. In contrast, the efficiency of cross-correlated relaxation pathways scales linearly with the overall correlation time of the molecule, which is related to its size. These new methods that exploit cross-correlated relaxation as a tool for structure determination should allow the characterization of conformations for larger RNA molecules, for which purpose J-coupling analysis is not feasible anymore.

25. Pf1-phage is commercially available (ASLA Biotech Ltd., Riga, Latvia). The phage solution can be exchanged into the NMR buffer by pelleting the phage in an ultracentrifuge (50K for 6 hours) and resuspending in NMR buffer multiple times. Prior to use, the phage should be spun down and resuspended by gently shaking for 6 hours with the RNA sample used in the isotropic experiments.

26. It does not appear that there will be a simple and quick procedure for NMR assignment of RNA molecules. Neglecting the problems with sensitivity or overlap, complete assignment requires a large number of experiments, if all of the optimized sequences are performed (~4 experiments for the bases, ~3 experiments to correlate the base resonances to the ribose, and ~2–3 experiments to correlate the ribose resonances). This results in a very rough estimate of about 20 days measurement time (assuming on average 2 days measurement time per experiment) for a RNA sample, with sample concentrations in the mM range and a molecular weight between 10 and 25 kDa, carried out on spectrometers with at least 500 MHz (proton resonance frequency). The subsequent data analysis and structure elucidation tends to be even more time consuming due to the absence of robust, automated procedures so that a complete RNA structure analysis using procedures reviewed here can not be accomplished in less than 2 month.

Acknowledgments

The authors thank S. Daudenarde and G. Pérez-Alvarado for invaluable discussions. This work was supported by the National Institutes of Health (AI040187 and GM66669, to M.H.).

References

1. Leulliot, N., Varani, G. (2001) Current topics in RNA-protein recognition: control of specificity and biological function through induced fit and conformational capture. *Biochemistry* 40, 7947–7956.
2. Williamson, J. R. (2000) Induced fit in RNA-protein recognition. *Nat Struct Biol* 7, 834–837.
3. Milligan, J. F., Groebe, D. R., Witherell, G. W., et al. (1987) Oligoribonucleotide synthesis using T7 RNA polymerase and synthetic DNA templates. *Nucleic Acids Res* 15, 8783–8798.
4. Milligan, J. F., Uhlenbeck, O. C. (1989) Synthesis of small RNAs using T7 RNA polymerase. *Methods Enzymol* 180, 51–62.
5. Perez-Canadillas, J. M., Varani, G. (2001) Recent advances in RNA-protein recognition. *Curr Opin Struct Biol* 11, 53–58.
6. Batey, R. T., Battiste, J. L., Williamson, J. R. (1995) Preparation of isotopically enriched RNAs for heteronuclear NMR. *Methods Enzymol* 261, 300–322.
7. Batey, R. T., Cloutier, N., Mao, H., et al. (1996) Improved large scale culture of *Methylophilus methylotrophus* for 13C/15N labeling and random fractional deuteration of ribonucleotides. *Nucleic Acids Res* 24, 4836–4837.
8. Batey, R. T., Inada, M., Kujawinski, E., et al. (1992) Preparation of isotopically labeled ribonucleotides for multidimensional NMR spectroscopy of RNA. *Nucleic Acids Res* 20, 4515–4523.
9. Nikonowicz, E. P., Sirr, A., Legault, P., et al. (1992) Preparation of 13C and 15N labelled RNAs for heteronuclear multidimensional NMR studies. *Nucleic Acids Res* 20, 4507–4513.
10. Zidek, L., Stefl, R., Sklenar, V. (2001) NMR methodology for the study of nucleic acids. *Curr Opin Struct Biol* 11, 275–281.
11. Cromsigt, J., van Buuren, B., Schleucher, J., et al. (2001) Resonance assignment and structure determination for RNA. *Methods Enzymol* 338, 371–399.
12. Furtig, B., Richter, C., Wohnert, J., et al. (2003) NMR spectroscopy of RNA. *Chembiochem* 4, 936–962.
13. Latham, M. P., Brown, D. J., McCallum, S. A., et al. (2005) NMR methods for studying the structure and dynamics of RNA. *Chembiochemistry* 6, 1492–1505.
14. Wu, H., Finger, L. D., Feigon, J. (2005) Structure determination of protein/RNA complexes by NMR. *Methods Enzymol* 394, 525–545.
15. Bax, A., Kontaxis, G., Tjandra, N. (2001) Dipolar couplings in macromolecular structure determination. *Methods Enzymol* 339, 127–174.
16. Hansen, M. R., Mueller, L., Pardi, A. (1998) Tunable alignment of macromolecules by filamentous phage yields dipolar coupling interactions. *Nat Struct Biol* 5, 1065–1074.
17. Tjandra, N., Bax, A. (1997) Direct measurement of distances and angles in biomolecules by NMR in a dilute liquid crystalline medium. *Science* 278, 1111–1114.
18. Reif, B., Hennig, M., Griesinger, C. (1997) Direct measurement of angles between bond vectors in high-resolution NMR. *Science* 276, 1230–1233.
19. Schwalbe, H., Carlomagno, T., Hennig, M., et al. (2001) Cross-correlated relaxation for measurement of angles between tensorial interactions. *Methods Enzymol* 338, 35–81.
20. Dingley, A. J., Grzesiek, S. (1998) Direct observation of hydrogen bonds in nucleic acid base pairs by internucleotide (2)J(NN) couplings. *J Am Chem Soc* 120, 8293–8297.
21. Pervushin, K., Ono, A., Fernandez, C., et al. (1998) NMR scaler couplings across Watson-Crick base pair hydrogen bonds in DNA observed by transverse relaxation optimized spectroscopy. *Proc Natl Acad Sci U S A* 95, 14147–14151.
22. Churcher, M. J., Lamont, C., Hamy, F., et al. (1993) High affinity binding of TAR RNA by the human immunodeficiency virus type-1 tat protein requires base-pairs in the RNA stem and amino acid residues

flanking the basic region. *J Mol Biol* 230, 90–110.

23. Long, K. S., Crothers, D. M. (1995) Interaction of human immunodeficiency virus type 1 Tat-derived peptides with TAR RNA. *Biochemistry* 34, 8885–8895.
24. Tao, J., Frankel, A. D. (1992) Specific binding of arginine to TAR RNA. *Proc Natl Acad Sci U S A* 89, 2723–2726.
25. Tao, J., Frankel, A. D. (1993) Electrostatic interactions modulate the RNA-binding and transactivation specificities of the human immunodeficiency virus and simian immunodeficiency virus Tat proteins. *Proc Natl Acad Sci U S A* 90, 1571–1575.
26. Puglisi, J. D., Chen, L., Frankel, A. D., et al. (1993) Role of RNA structure in arginine recognition of TAR RNA. *Proc Natl Acad Sci U S A* 90, 3680–3684.
27. Puglisi, J. D., Tan, R., Calnan, B. J., et al. (1992) Conformation of the TAR RNA-arginine complex by NMR spectroscopy. *Science* 257, 76–80.
28. Aboul-ela, F., Karn, J., Varani, G. (1995) The structure of the human immunodeficiency virus type-1 TAR RNA reveals principles of RNA recognition by Tat protein. *J Mol Biol* 253, 313–332.
29. Brodsky, A. S., Williamson, J. R. (1997) Solution structure of the HIV-2 TAR-argininamide complex. *J Mol Biol* 267, 624–639.
30. Aboul-ela, F., Karn, J., Varani, G. (1996) Structure of HIV-1 TAR RNA in the absence of ligands reveals a novel conformation of the trinucleotide bulge. *Nucleic Acids Res* 24, 3974–3781.
31. Long, K. S., Crothers, D. M. (1999) Characterization of the solution conformations of unbound and Tat peptide-bound forms of HIV-1 TAR RNA. *Biochemistry* 38, 10059–10069.
32. Sambrook, J., Fritsch, E. F., Maniatis, T. (1989) *Molecular Cloning: A Laboratory Manual*, Cold Spring Harbor Laboratory Press, Cold Spring Harbor, NY.
33. Yin, Y., Carter, C. W., Jr. (1996) Incomplete factorial and response surface methods in experimental design: yield optimization of tRNA(Trp) from in vitro T7 RNA polymerase transcription. *Nucleic Acids Res* 24, 1279–1286.
34. Wyatt, J. R., Chastain, M., Puglisi, J. D. (1991) Synthesis and purification of large amounts of RNA oligonucleotides. *Biotechniques* 11, 764–769.
35. Anderson, A. C., Scaringe, S. A., Earp, B. E., et al. (1996) HPLC purification of RNA for crystallography and NMR. *RNA* 2, 110–117.
36. Shields, T. P., Mollova, E., Ste Marie, L., et al. (1999) High-performance liquid chromatography purification of homogenous-length RNA produced by trans cleavage with a hammerhead ribozyme. *RNA* 5, 1259–1267.
37. Wuthrich, K. (1986) *NMR of Proteins and Nucleic Acids*, Wiley, New York.
38. Nikonowicz, E. P., Pardi, A. (1992) Three-dimensional heteronuclear NMR studies of RNA. *Nature* 355, 184–186.
39. Nikonowicz, E. P., Pardi, A. (1993) An efficient procedure for assignment of the proton, carbon and nitrogen resonances in 13C/15N labeled nucleic acids. *J Mol Biol* 232, 1141–1156.
40. Wijmenga, S. S., van Buuren, B. N. M. (1998) The use of NMR methods for conformational studies of nucleic acids. *Prog Nucl Magn Reson Spectrosc* 32, 287–387.
41. Zhou, H., Vermeulen, A., Jucker, F. M., et al. (1999) Incorporating residual dipolar couplings into the NMR solution structure determination of nucleic acids. *Biopolymers* 52, 168–180.
42. Hansen, M. R., Hanson, P., Pardi, A. (2000) Filamentous bacteriophage for aligning RNA, DNA, and proteins for measurement of nuclear magnetic resonance dipolar coupling interactions. *Methods Enzymol* 317, 220–240.
43. Meiler, J., Prompers, J. J., Peti, W., et al. (2001) Model-free approach to the dynamic interpretation of residual dipolar couplings in globular proteins. *J Am Chem Soc* 123, 6098–6107.
44. Peti, W., Meiler, J., Bruschweiler, R., et al. (2002) Model-free analysis of protein backbone motion from residual dipolar couplings. *J Am Chem Soc* 124, 5822–5833.
45. Tolman, J. R. (2002) A novel approach to the retrieval of structural and dynamic information from residual dipolar couplings using several oriented media in biomolecular NMR spectroscopy. *J Am Chem Soc* 124, 12020–12030.
46. Lippens, G., Dhalluin, C., Wieruszeski, J. M. (1995) Use of a Water Flip-Back Pulse in the Homonuclear Noesy Experiment. *J Biomol Nmr* 5, 327–331.
47. Peterson, R. D., Theimer, C. A., Wu, H. H., et al. (2004) New applications of 2D filtered/edited NOESY for assignment and

structure elucidation of RNA and RNA-protein complexes. *J Biomol Nmr* 28, 59–67.

48. Duchardt, E., Richter, C., Reif, B., et al. (2001) Measurement of 2J(H,C)- and 3J(H,C)-coupling constants by alpha/beta selective HC(C)H-TOCSY. *J Biomol NMR* 21, 117–126.
49. Schwalbe, H., Marino, J. P., Glaser, S. J., et al. (1995) Measurement of H,H-Coupling Constants Associated with nu1, nu2, and nu3 in Uniformly 13C-Labeled RNA by HCC-TOCSY-CCH-E.COSY *J Am Chem Soc* 117, 7251–7252.
50. Schwalbe, H., Marino, J. P., King, G. C., et al. (1994) Determination of a complete set of coupling constants in 13C-labeled oligonucleotides. *J Biomol NMR* 4, 631–644.
51. Hines, J. V., Varani, G., Landry, S. M., et al. (1993) The stereospecific assignment of H5′ and H5″ in RNA using the sign of two-bond carbon-proton scalar coupling. *J Am Chem Soc* 115, 11002–11003.
52. Trantirek, L., Stefl, R., Masse, J. E., et al. (2002) Determination of the glycosidic torsion angles in uniformly C-13-labeled nucleic acids from vicinal coupling constants (3)J(C2/4-H1′) and (3)J(C6/8-H1′). *J Biomol NMR* 23, 1–12.
53. Carlomagno, T., Hennig, M., Williamson, J. R. (2002) A novel PH-cT-COSY methodology for measuring JPH coupling constants in unlabeled nucleic acids. application to HIV-2 TAR RNA. *J Biomol NMR* 22, 65–81.
54. Sklenar, V., Miyashiro, H., Zon, G., et al. (1986) Assignment of the 31P and 1H resonances in oligonucleotides by two-dimensional NMR spectroscopy. *FEBS Lett* 208, 94–98.
55. Schwalbe, H., Samstag, W., Engels, J. W., et al. (1993) Determination of 3J(C,P) and 3J(H,P) coupling constants in nucleotide oligomers with FIDS-HSQC. *J Biomol NMR* 3, 479–486.
56. Hoogstraten, C. G., Pardi, A. (1998) Measurement of carbon-phosphorus J coupling constants in RNA using spin-echo difference constant-time HCCH-COSY. *J Magn Reson* 133, 236–240.
57. Legault, P., Jucker, F. M., Pardi, A. (1995) Improved measurement of 13C, 31P J coupling constants in isotopically labeled RNA. *FEBS Lett* 362, 156–160.
58. Szyperski, T., Fernandez, C., Ono, A., et al. (1999) The 2D [31P] spin-echo-difference constant-time [13C, 1H]-HMQC experiment for simultaneous determination of 3J(H3′P) and 3J(C4′P) in 13C-labeled nucleic acids and their protein complexes. *J Magn Reson* 140, 491–494.
59. Hu, W., Bouaziz, S., Skripkin, E., et al. (1999) Determination of 3J(H3i, Pi+1) and 3J(H5i/5i, Pi) coupling constants in 13C-labeled nucleic acids using constant-time HMQC. *J Magn Reson* 139, 181–185.
60. Clore, G. M., Murphy, E. C., Gronenborn, A. M., et al. (1998) Determination of three-bond 1H3′-31P couplings in nucleic acids and protein-nucleic acid complexes by quantitative J correlation spectroscopy. *J Magn Reson* 134, 164–167.
61. Gotfredsen, C. H., Meissner, A., Duus, J. O., et al. (2000) New methods for measuring 1H-31P coupling constants in nucleic acids. *Magn Reson Chem* 38, 692–695.
62. Richter, C., Reif, B., Worner, K., et al. (1998) A new experiment for the measurement of nJ(C,P) coupling constants including 3J(C4′i,Pi) and 3J(C4′i,Pi+1) in oligonucleotides. *J Biomol NMR* 12, 223–230.
63. Legault, P., Pardi, A. (1994) 31P chemical shift as a probe of structural motifs in RNA. *J Magn Reson B* 103, 82–86.
64. Richter, C., Reif, B., Griesinger, C., et al. (2000) NMR spectroscopic determination of angles and in RNA from CH-dipolar coupling, P-CSA cross-correlated relaxation. *J Am Chem Soc* 122, 12728–12731.
65. Duchardt, E., Richter, C., Ohlenschlager, O., et al. (2004) Determination of the glycosidic bond angle chi in RNA from cross-correlated relaxation of CH dipolar coupling and N chemical shift anisotropy. *J Am Chem Soc* 126, 1962–1970.
66. Ravindranathan, S., Kim, C. H., Bodenhausen, G. (2003) Cross correlations between 13C-1H dipolar interactions and 15N chemical shift anisotropy in nucleic acids. *J Biomol NMR* 27, 365–375.
67. Felli, I. C., Richter, C., Griesinger, C., et al. (1999) Determination of RNA sugar pucker mode from cross-correlated relaxation in solution NMR spectroscopy. *J Am Chem Soc* 121, 1956–1957.
68. Richter, C., Griesinger, C., Felli, I., et al. (1999) Determination of sugar conformation in large RNA oligonucleotides from analysis of dipole-dipole cross correlated relaxation by solution NMR spectroscopy. *J Biomol NMR* 15, 241–250.
69. Andersson, P., Weigelt, J., Otting, G. (1998) Spin-state selection filters for the measurement of heteronuclear one-bond coupling constants. *J Biomol NMR* 12, 435–441.

70. Tjandra, N., Bax, A. (1997) Measurement of dipolar contributions to 1JCH splittings from magnetic-field dependence of J modulation in two-dimensional NMR spectra. *J Magn Reson* 124, 512–515.
71. Tjandra, N., Grzesiek, S., Bax, A. (1996) Magnetic field dependence of nitrogen-proton J splittings in N-15-enriched human ubiquitin resulting from relaxation interference and residual dipolar coupling. *J Am Chem Soc* 118, 6264–6272.
72. Hennig, M., Carlomagno, T., Williamson, J. R. (2001) Residual dipolar coupling TOCSY for direct through space correlations of base protons and phosphorus nuclei in RNA. *J Am Chem Soc* 123, 3395–3396.
73. Wu, Z., Tjandra, N., Bax, A. (2001) Measurement of 1H3′-31P dipolar couplings in a DNA oligonucleotide by constant-time NOESY difference spectroscopy. *J Biomol NMR* 19, 367–370.
74. Wu, Z., Tjandra, N., Bax, A. (2001) 31P chemical shift anisotropy as an aid in determining nucleic acid structure in liquid crystals. *J Am Chem Soc* 123, 3617–3618.
75. Dingley, A. J., Masse, J. E., Feigon, J., et al. (2000) Characterization of the hydrogen bond network in guanosine quartets by internucleotide 3hJ(NC)′ and 2hJ(NN) scalar couplings. *J Biomol NMR* 16, 279–289.
76. Dingley, A. J., Masse, J. E., Peterson, R. D., et al. (1999) Internucleotide scalar couplings across hydrogen bonds in Watson-Crickand Hoogsteen base pairs of a DNA triplex. *J Am Chem Soc* 121, 6019–6027.
77. Hennig, M., Williamson, J. R. (2000) Detection of N-H…N hydrogen bonding in RNA via scalar couplings in the absence of observable imino proton resonances. *Nucleic Acids Res* 28, 1585–1593.
78. Liu, A. Z., Majumdar, A., Hu, W. D., et al. (2000) NMR detection of N-H…O=C hydrogen bonds in C-13,N-15-labeled nucleic acids. *J Am Chem Soc* 122, 3206–3210.
79. Majumdar, A., Kettani, A., Skripkin, E. (1999) Observation and measurement of internucleotide 2JNN coupling constants between 15N nuclei with widely separated chemical shifts. *J Biomol NMR* 14, 67–70.
80. Majumdar, A., Kettani, A., Skripkin, E., et al. (1999) Observation of internucleotide NH…N hydrogen bonds in the absence of directly detectable protons. *J Biomol NMR* 15, 207–2-11.
81. Wohnert, J., Ramachandran, R., Gorlach, M., et al. (1999) Triple-resonance experiments for correlation of H5 and exchangeable pyrimidine base hydrogens in (13)C,(15) N-labeled RNA. *J Magn Reson* 139, 430–433.
82. Sklenar, V., Peterson, R. D., Rejante, M. R., et al. (1994) Correlation of nucleotide base and sugar protons in a N-15-labeled Hiv-1 RNA oligonucleotide by H-1-N-15 Hsqc experiments. *J Biomol NMR* 4, 117–122.
83. Fohrer, J., Hennig, M., Carlomagno, T. (2006) Influence of the 2′-hydroxyl group conformation on the stability of A-form helices in RNA. *J Mol Biol* 356, 280–287.
84. Hennig, M., Fohrer, J., Carlomagno, T. (2005) Assignment and NOE analysis of 2′-hydroxyl protons in RNA: implications for stabilization of RNA A-form duplexes. *J Am Chem Soc* 127, 2028–2029.
85. Giedroc, D. P., Cornish, P. V., Hennig, M. (2003) Detection of scalar couplings involving 2′-hydroxyl protons across hydrogen bonds in a frameshifting mRNA pseudoknot. *J Am Chem Soc* 125, 4676–4677.
86. Simorre, J. P., Zimmermann, G. R., Mueller, L., et al. (1996) Correlation of the guanosine exchangeable and nonexchangeable base protons in 13C-/15N-labeled RNA with an HNC-TOCSY-CH experiment. *J Biomol NMR* 7, 153–156.
87. Simorre, J. P., Zimmermann, G. R., Mueller, L., et al. (1996) Triple-resonance experiments for assignment of adenine base resonances in C-13/N-15-labeled RNA. *J Am Chem Soc* 118, 5316–5317.
88. Simorre, J. P., Zimmermann, G. R., Pardi, A., et al. (1995) Triple resonance HNCCCH experiments for correlating exchangeable and nonexchangeable cytidine and uridine base protons in RNA. *J Biomol NMR* 6, 427–432.
89. Sklenar, V., Dieckmann, T., Butcher, S. E., et al. (1996) Through-bond correlation of imino and aromatic resonances in C-13-,N-15-labeled RNA via heteronuclear TOCSY. *J Biomol Nmr* 7, 83–87.
90. Wohnert, J., Gorlach, M., Schwalbe, H. (2003) Triple resonance experiments for the simultaneous correlation of H6/H5 and exchangeable protons of pyrimidine nucleotides in C-13, N-15-labeled RNA applicable to larger RNA molecules. *J Biomol Nmr* 26, 79–83.
91. Fiala, R., Jiang, F., Patel, D. J. (1996) Direct correlation of exchangeable and non-exchangeable protons on purine bases in 13C,15N-labeled RNA using a HCCNH-TOCSY experiment. *J Am Chem Soc* 118, 689–690.
92. Simon, B., Zanier, K., Sattler, M. (2001) A TROSY relayed HCCH-COSY experiment

for correlating adenine H2/H8 resonances in uniformly 13C-labeled RNA molecules. *J Biomol NMR* 20, 173–176.

93. Legault, P., Farmer, B. T., Mueller, L., et al. (1994) Through-bond correlation of adenine protons in a C-13-labeled ribozyme. *J Am Chem Soc* 116, 2203–2204.
94. Marino, J. P., Prestegard, J. H., Crothers, D. M. (1994) Correlation of adenine H2/H8 resonances in uniformly C-13 labeled Rnas by 2d Hcch-Tocsy: a new tool for H-1 assignment. *J Am Chem Soc* 116, 2205–2206.
95. Marino, J. P., Diener, J. L., Moore, P. B., et al. (1997) Multiple-quantum coherence dramatically enhances the sensitivity of CH and CH2 correlations in uniformly 13C-labeled RNA. *J Am Chem Soc* 119, 7361–7366.
96. Sklenar, V., Dieckmann, T., Butcher, S. E., et al. (1998) Optimization of triple-resonance HCN experiments for application to larger RNA oligonucleotides. *J Magn Reson* 130, 119–124.
97. Fiala, R., Czernek, J., Sklenar, V. (2000) Transverse relaxation optimized triple-resonance NMR experiments for nucleic acids. *J Biomol NMR* 16, 291–302.
98. Riek, R., Pervushin, K., Fernandez, C., et al. (2001) [(13)C,(13)C]- and [(13)C,(1)H]-TROSY in a triple resonance experiment for ribose-base and intrabase correlations in nucleic acids. *J Am Chem Soc* 123, 658–664.
99. Farmer, B. T., Muller, L., Nikonowicz, E. P., et al. (1993) Unambiguous resonance assignments in carbon-13, nitrogen-15-labeled nucleic acids by 3D triple-resonance NMR. *J Am Chem Soc* 115, 11040–11041.
100. Sklenar, V., Rejante, M. R., Peterson, R. D., et al. (1993) Two-dimensional triple-resonance HCNCH experiment for direct correlation of ribose H1′ and base H8, H6 protons in 13C,15N-labeled RNA oligonucleotides. *J Am Chem Soc* 115, 12181–12182.
101. Fesik, S. W., Eaton, H. L., Olejniczak, E. T., et al. (1990) 2D and 3D NMR spectroscopy employing carbon-13/carbon-13 magnetization transfer by isotropic mixing. Spin system identification in large proteins. *J Am Chem Soc* 112, 886–888.
102. Kay, L. E., Ikura, M., Bax, A. (1990) Proton-proton correlation via carbon-carbon couplings: a three-dimensional NMR approach for the assignment of aliphatic resonances in proteins labeled with carbon-13. *J Am Chem Soc* 112, 888–889.
103. Pardi, A. (1995) Multidimensional heteronuclear NMR experiments for structure determination of isotopically labeled RNA. *Methods Enzymol* 261, 350–380.
104. Pardi, A., Nikonowicz, E. P. (1992) Simple procedure for resonance assignment of the sugar protons in carbon-13 labeled RNAs. *J Am Chem Soc* 114, 9202–9203.
105. Hu, W., Kakalis, L. T., Jiang, L., et al. (1998) 3D HCCH-COSY-TOCSY experiment for the assignment of ribose and amino acid side chains in 13C labeled RNA and protein. *J Biomol NMR* 12, 559–564.
106. Glaser, S. J., Schwalbe, H., Marino, J. P., et al. (1996) Directed TOCSY, a method for selection of directed correlations by optimal combinations of isotropic and longitudinal mixing. *J Magn Reson B* 112, 160–180.
107. Kellogg, G. W. (1992) Proton-detected hetero-TOCSY experiments with application to nucleic acids. *J Magn Reson* 98, 176–182.
108. Kellogg, G. W., Szewczak, A. A., Moore, P. B. (1992) Two-dimensional hetero-TOCSY-NOESY. Correlation of phosphorus-31 resonances with anomeric and aromatic proton resonances in RNA. *J Am Chem Soc* 114, 2727–2728.
109. Kellogg, G. W., Schweitzer, B. I. (1993) Two- and three-dimensional 31P-driven NMR procedures for complete assignment of backbone resonances in oligodeoxyribonucleotides. *J Biomol NMR* 3, 577–595.
110. Heus, H. A., Wijmenga, S. S., Vandeven, F. J. M., et al. (1994) Sequential backbone assignment in C-13-labeled Rna via through-bond coherence transfer using 3-dimensional triple-resonance spectroscopy (H-1, C-13, P-31) and 2-dimensional hetero Tocsy. *J Am Chem Soc* 116, 4983–4984.
111. Marino, J. P., Schwalbe, H., Anklin, C., et al. (1994) A 3-dimensional triple-resonance H-1,C-13,P-31 experiment: sequential through-bond correlation of ribose protons and intervening phosphorus along the Rna oligonucleotide backbone. *J Am Chem Soc* 116, 6472–6473.
112. Marino, J. P., Schwalbe, H., Anklin, C., et al. (1995) Sequential correlation of anomeric ribose protons and intervening phosphorus in RNA oligonucleotides by a 1H, 13C, 31P triple resonance experiment: HCP-CCH-TOCSY. *J Biomol NMR* 5, 87–92.
113. Wijmenga, S. S., Heus, H. A., Leeuw, H. A., et al. (1995) Sequential backbone assignment of uniformly 13C-labeled RNAs by a two-dimensional P(CC)H-TOCSY triple resonance NMR experiment. *J Biomol NMR* 5, 82–86.

114. Marino, J. P., Schwalbe, H., Griesinger, C. (1999) J-coupling restraints in RNA structure determination. *Acc Chem Res* 32, 614–623.
115. Schwieters, C. D., Kuszewski, J. J., Tjandra, N., et al. (2003) The Xplor-NIH NMR molecular structure determination package. *J Magn Reson* 160, 65–73.
116. Brunger, A. T., Adams, P. D., Clore, G. M., et al. (1998) Crystallography & NMR system: A new software suite for macromolecular structure determination. *Acta Crystallographica Section D-Biological Crystallography* 54, 905–921.
117. Stein, E. G., Rice, L. M., Brunger, A. T. (1997) Torsion-angle molecular dynamics as a new efficient tool for NMR structure calculation. *J Magn Reson* 124, 154–164.
118. Pearlman, D. A., Case, D. A., Caldwell, J. W., et al. (1995) AMBER, a computer program for applying molecular mechanics, normal mode analysis, molecular dynamics and free energy calculations to elucidate the structures and energies of molecules. *Computer Physics Communications* 91, 1–41.
119. Tsui, V., Case, D. A. (2000) Molecular dynamics simulations of nucleic acids with a generalized born solvation model. *J Am Chem Soc* 122, 2489–2498.
120. Clore, G. M., Garrett, D. S. (1999) R-factor, free R, and complete cross-validation for dipolar coupling refinement of NMR structures. *J Am Chem Soc* 121, 9008–9012.
121. Clore, G. M., Kuszewski, J. (2003) Improving the accuracy of NMR structures of RNA by means of conformational database potentials of mean force as assessed by complete dipolar coupling cross-validation. *J Am Chem Soc* 125, 1518–1525.
122. Cromsigt, J. A., Hilbers, C. W., Wijmenga, S. S. (2001) Prediction of proton chemical shifts in RNA. Their use in structure refinement and validation. *J Biomol NMR* 21, 11–29.
123. Baklanov, M. M., Golikova, L. N., Malygin, E. G. (1996) Effect on DNA transcription of nucleotide sequences upstream to T7 promoter. *Nucleic Acids Res* 24, 3659–3660.
124. Moran, S., Ren, R. X., Sheils, C. J., et al. (1996) Non-hydrogen bonding 'terminator' nucleosides increase the 3′-end homogeneity of enzymatic RNA and DNA synthesis. *Nucleic Acids Res* 24, 2044–2052.
125. Ferre-D'Amare, A. R., Doudna, J. A. (1996) Use of cis- and trans-ribozymes to remove 5′ and 3′ heterogeneities from milligrams of in vitro transcribed RNA. *Nucleic Acids Res* 24, 977–978.
126. Price, S. R., Ito, N., Oubridge, C., et al. (1995) Crystallization of RNA-protein complexes. I. Methods for the large-scale preparation of RNA suitable for crystallographic studies. *J Mol Biol* 249, 398–408.
127. Scott, L. G., Tolbert, T. J., Williamson, J. R. (2000) Preparation of specifically 2H- and 13C-labeled ribonucleotides. *Methods Enzymol* 317, 18–38.
128. Sklenar, V., Brooks, B. R., Zon, G., et al. (1987) Absorption mode two-dimensional NOE spectroscopy of exchangeable protons in oligonucleotides. *FEBS Lett* 216, 249–252.
129. Rance, M., Sorensen, O. W., Bodenhausen, G., et al. (1983) Improved spectral resolution in cosy 1H NMR spectra of proteins via double quantum filtering. *Biochem Biophys Res Commun* 117, 479–485.

http://www.springer.com/978-1-58829-707-5

Bioinformatics
Volume I: Data, Sequence Analysis and Evolution
Keith, J.M. (Ed.)
2008, XII, 562 p. 136 illus., 3 illus. in color., Hardcover
ISBN: 978-1-58829-707-5
A product of Humana Press